Multipole approximation of special nonlinear magnets for the IOTA ring.

Viktor Vorobev*

Physical Faculty of St. Petersburg State University, St. Petersburg 198504, Russia

(Dated: September 9, 2013)

I. INTRODUCTION

All existing focusing optics for accelerators are built to be "linear", i.e. the transverse focusing force is proportional to the particle displacement from the closed orbit. Such approach is used in order to make trajectories stable in the entire area of phase space, because the potential describing linear focusing is integrable and does not produce chaotic motion. Technically, the needed field is achieved with the help of dipole and quadrupole magnets. But the linear motion is unstable to perturbations in the focusing fields and excludes any betatron tune spread over particle's energy, which is beneficial for the beam stability. Moreover, the focusing strength depends on the particle's energy deviation from the designed one. These undesired effects are usually suppressed by the addition of non-linear elements, such as sextupoles and octupoles. Unfortunately, these additions make focusing potential nonintegrabe, leading to the limitation of stable phase space area.

Recent research showed, that there exist non-linear potentials that, nevertheless, are fully integrable [1, 2]. Thus, there is an opportunity to create stable non-linear focusing optics that provides high betatron tune spread and mitigate magnetic field errors. This approach is to be implemented in electron storage ring called Integrable Optics Test Accelerator (IOTA) at Fermilab [3]. The main goal is to show the possibility to implement the nonlinear integrable system in a realistic accelerator design.

Development of a magnet, which creates exact non-linear potential, is a technically complicated task, that takes much time and efforts. However, it is possible to expand the non-linear potential into superposition of multipoles of even orders (i.e quadrupole, octupole, etc.). Though this series is not convergent in the entire space, a few low order terms can

* vorobjovvictor@gmail.com; vorobev@fnal.gov

Operated by Fermi Research Alliance, LLC under Contract No. De-AC02-07CH11359 with the United States Department of Energy.

be used to model the true potential in some limited area. In turn, each of the multipole potentials can be generated by specified electrical current in PCB coiled on the surface of storage ring's vacuum tube. Such approach is much cheaper than the creation of a magnet of solid iron with high current coil and faster than the development of "exact" non-linear magnet, but it can help identify some features of non-linear integrable optics application.

The goal of this research work is to find analytically the angular distribution of electrical current on the surface of the vacuum tube, which creates inside it multipole potential with given parameters. Hereafter, there is the task to develop a model of flexible printed circuit board (PCB), which could be coiled around the vacuum tube in order to provide the desired current distribution.

II. COIL CURRENT

One of the mentioned non-linear integrable potentials [1] has the following form in elliptic coordinates:

$$U_N(x_N, y_N) = \frac{f_2(\xi) + g_2(\eta)}{\xi^2 - \eta^2}, \tag{1}$$

where the function in numerator has form

$$f_2(\xi) = \xi\sqrt{\xi^2 - 1}(d + t\,\mathrm{acosh}\xi), \tag{2}$$

$$g_2(\eta) = \eta\sqrt{1 - \eta^2}(q + t\,\mathrm{acos}\xi), \tag{3}$$

elliptic coordinates relate to Cartesian through

$$\xi = \frac{\sqrt{(x_N + c)^2 + y_N^2} + \sqrt{(x_N - c)^2 + y_N^2}}{2c}, \tag{4}$$

$$\eta = \frac{\sqrt{(x_N + c)^2 + y_N^2} - \sqrt{(x_N - c)^2 + y_N^2}}{2c}. \tag{5}$$

Here c, d, t and q are some arbitrary constants.

Real transverse coordinates (x, y) connected with normalized ones (x_N, y_N) through the beta-function

$$x_N = \frac{x}{\sqrt{\beta\,(s)}}, \qquad y_N = \frac{y}{\sqrt{\beta\,(s)}}. \tag{6}$$

Real potential in dimensional units is expressed through normalized one (1) as

$$U_0(x, y, s) = \frac{E}{\beta\,(s)} U_N\,(x_N, y_N)\,, \tag{7}$$

where E is particle's energy and s is longitudinal coordinate.

Further, the case when potential (1) can be presented as a superposition of even powers of $r_N = \sqrt{x_N^2 + y_N^2}$ ("even" multipoles) is considered. For this purpose we should put $d = 0$ in (2) and $q = -\pi t/2$ in (3), the the series at the point $r_N = 0$ has form

$$U_N(r_N, \varphi) = -\frac{t}{c^2}\left(r_N^2 \cos(2\varphi) + \frac{2}{3c^2} r_N^4 \cos(4\varphi) + \frac{8}{15c^4} r_N^6 \cos(6\varphi) + ...\right), \tag{8}$$

where $\varphi = \mathrm{atan}(y/x)$.

Quadrupole and octupole terms (proportional to r^2 and r^4) are taken for further consideration. In FIG. 1 the similarity of the initial potential and truncated one is shown. These two pictures are quite similar, relative difference between magnetic fields corresponding to the potentials is given below in FIG. 3.

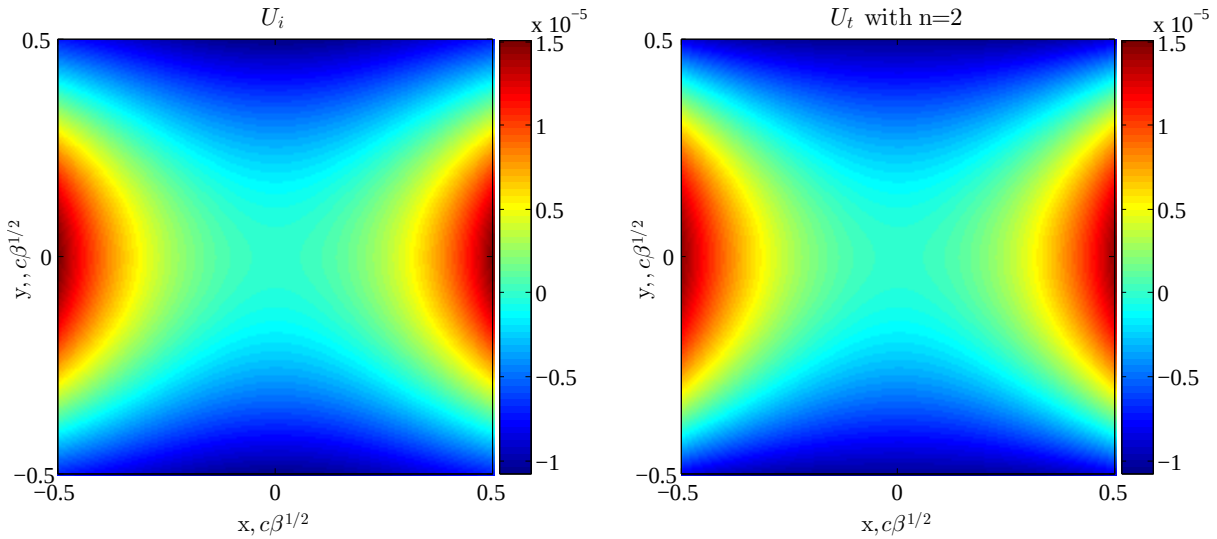

FIG. 1. Non-linear potential U_i given by equation (1) and truncated series U_t (8), consisting of the first two terms. Transverse coordinates are given in units $c\sqrt{\beta}$. Potentials are normalized to E/β.

So, we need to generate the truncated potential

$$U_t(r_n, \varphi) = -t\left(r_N^2 \cos(2\varphi) + \frac{2}{3c^2} r_N^4 \cos(4\varphi)\right) \tag{9}$$

inside the cylindrical vacuum tube of radius r_d with current distribution $I(\varphi)$ on its surface. Here and further t is normalized to c^2.

In order to determine the magnetic field by given potential the following formulae are used

$$\vec{F} = -\vec{\nabla} U_t(r_N, \varphi), \tag{10}$$

$$\vec{F} = q\vec{v} \times \vec{B}, \tag{11}$$

where $\vec{\nabla}$ is gradient over normalized coordinates, $\vec{v} = v\vec{e}_z$ is velocity of the particle. Thus, we have

$$B_x = \frac{1}{qv} t \left(-2y_N + \frac{8}{3c^2} \left(y_N^3 - 3y_N x_N^2 \right) \right), \qquad B_y = -\frac{1}{qv} t \left(2x_N + \frac{8}{3c^2} \left(x_N^3 - 3x_N y_N^2 \right) \right). \tag{12}$$

Figures 2 and 3 show, that the difference between fields of initial non-linear potential and chosen truncated series is insignificant and less than 1% inside some circular area.

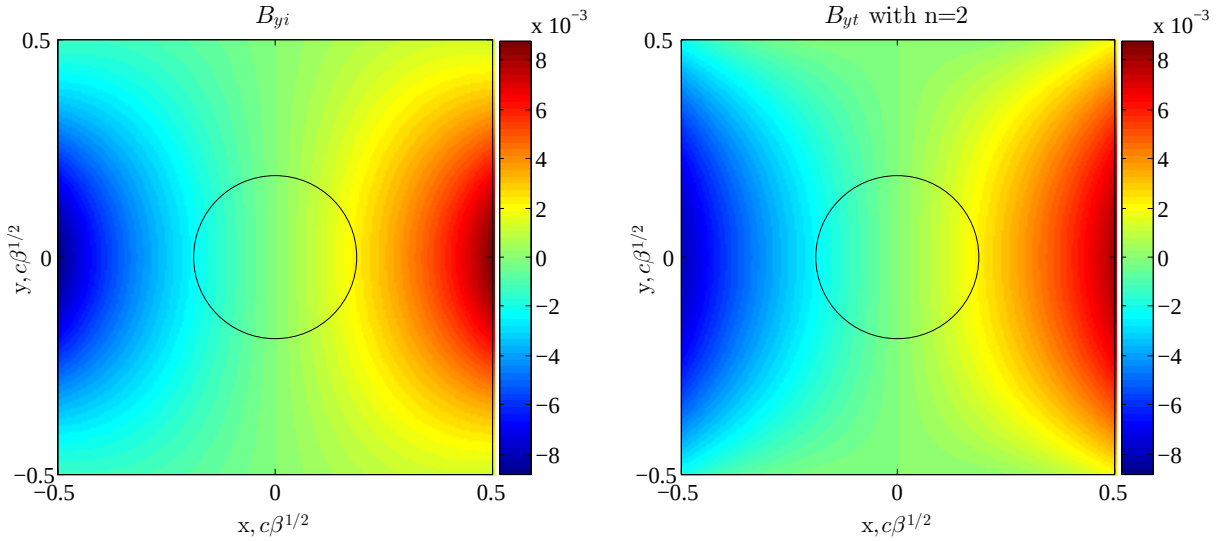

FIG. 2. Component B_{yi} produced by non-linear potential (1) and B_{yt} produced by truncated one (8), consisting of the first two terms. Transverse coordinates are given in units $c\sqrt{\beta}$. Magnetic field is normalized to $E/(qv\beta)$. Inside black circle the relative difference is less than 1%.

For convenience, the complex field is introduced by the following way

$$\mathbf{B}(\mathbf{z_N}) = B_y(x_N, y_N) + iB_x(x_N, y_N), \qquad \mathbf{z_N} = x_N + iy_N, \tag{13}$$

then we get following multipole expansion

$$\mathbf{B}(\mathbf{z_N}) = -\frac{2t}{qv}\mathbf{z_N} - \frac{8t}{3qvc^2}\mathbf{z_N^3} = B_2\mathbf{z_N} + B_4\mathbf{z_N^3}. \tag{14}$$

The complex field in the region inside the circular current shell can be expressed as

$$\mathbf{B}(\mathbf{z_N}) = -\left(\frac{\mu_0}{2\pi r_{dN}}\right) \int_0^{2\pi} \sum_{m=2,4} \left(\frac{\mathbf{z_N}}{r_{dN}}\right)^{m-1} \exp(-im\varphi) I(\varphi) d\varphi, \tag{15}$$

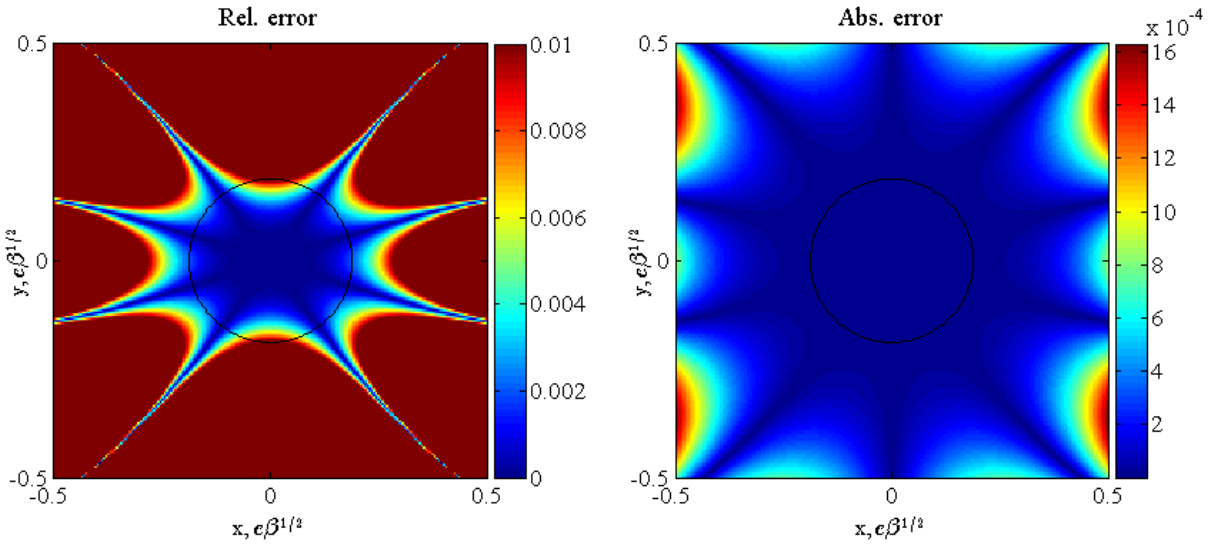

FIG. 3. Relative and absolute difference between value displayed in FIG. 2. Transverse coordinates are given in units $c\sqrt{\beta}$, absolute discrepancy is in $E/(qv\beta)$ units. Inside black circle the relative difference is less than 1%.

$$I(\varphi) = I_2 \cos(2\varphi) + I_4 \cos(4\varphi). \tag{16}$$

Thus, we get the relation between amplitudes of the current and multipole expansion (14)

$$B_m = -\frac{\mu_0 I_m}{2r_{dN}^m}. \tag{17}$$

Finally, for the current we have

$$I_2 = \frac{4tr_{dN}^2}{q\mu_0 v}, \qquad I_4 = \frac{16tr_{dN}^4}{3q\mu_0 v c^2}. \tag{18}$$

$$I = \frac{4tr_{dN}^2}{q\mu_0 v}\cos(2\varphi) + \frac{16tr_{dN}^4}{3q\mu_0 v c^2}\cos(4\varphi). \tag{19}$$

For technical purposes it is more convenient to have a representation for current in dimensional units and real coordinates. So, using (6) and (7)

$$I_0(\varphi) = \frac{E}{qZ_0}\frac{\gamma}{\sqrt{\gamma^2-1}}\frac{4t}{\beta^2}\left(r_d^2\cos(2\varphi) + \frac{4}{3\beta c^2}r_d^4\cos(4\varphi)\right), \tag{20}$$

where γ is Lorentz-factor, $Z_0 = 120\pi\ \Omega$ is vacuum impedance.

III. COIL DESIGN

In order to get specific values of the current (20) on the vacuum tube, some parameters of the IOTA design are needed (see TABLE I). Among them are the constants from the initial

potential, which are chosen for the development of "exact" non-linear magnet. But not all these parameters are fixed and can be slightly varied in order to develop a more realistic PCB coil powered with 2A current.

TABLE I. Some IOTA design parameters

Parameter	**Sign**	**Value**	**Can change?**
Particles'energy	E	150 MeV	fixed
Vacuum tube radius	r_d	1 inch	may vary
Minimum beta-function	β	0.7 m	fixed
Constant c	c	0.01 $\sqrt{\text{m}}$	may vary
Constant t	t	0.1 - 0.5	
Source of current	I_{max}	2 A	may be less

For the values shown in TAB. I (t = 0.5) the peak values of "quadrupole" and "octupole" currents in representation (16) are $I_2 = 1.0478 \cdot 10^3$A and $I_2 = 1.2876 \cdot 10^4$A correspondingly. Such current presupposes large number of PCB turns, which is unacceptable.

A special program was created that "generates" appropriate coil and calculates the number of its turns by given parameters (such as radius of the tube, constants and maximum current in one coil's wire). Program is based on the following principle: the sector of π/n (where n is the order of the term) is divided in 5 sections and each section is filled with wires so that the total current is equal to the theoretical current in this section. Then these wires are separated into layers with respect to the maximum number of wires in one section in one layer. But calculations showed, that it is very hard to stay close to the initial parameters (TAB. I) and get the number of turns low at the same moment. So, it was decided to eliminate quadrupole coil and use only octupole. This step is conditioned by previous simulations of the beam dynamics, that showed particles are stable in the field of octupole magnets [4].

Parameters of one of the coils are presented in TABLE II. Values in TABLE III represent the distribution of wires in the arc of the tube equal $r_d\frac{\pi}{4} = 10\ mm$ (sector). This is visualized in FIG. 5. The whole turn represent alternating (currents of different signs) sequence of sectors in amount of 4 each sign (see FIG. 4). Other octupole coils for different parameters are given in TABLE IV.

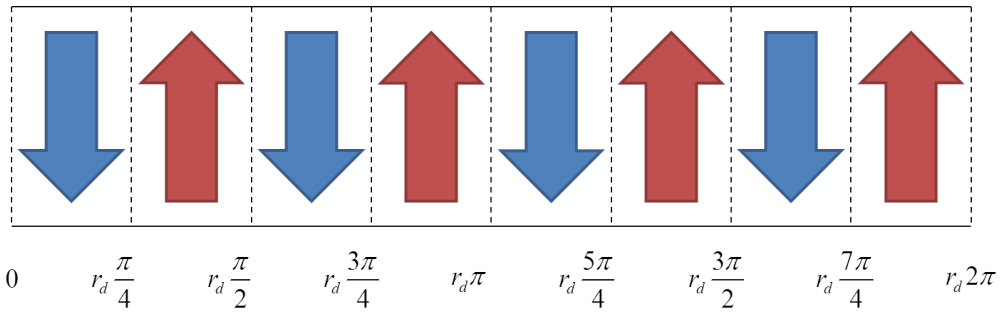

FIG. 4. Sequence of sectors with current of different signs in one layer for octupole coil.

As one can see, the current of one wire is equal to 0.37 Amperes which corresponds to relatively high current density in copper (42 A/mm^2). It is obvious, that the cooling of internal layers of the coil is the most difficult task in such situation. So, in order to determine whether such current would cause wire fusion, a specialized free-software [5] was used. It allows on the base of parameters of multilayered PCB estimate temperature rise for both internal and external layers. Calculations made for coil model presented above show, that for current equal 0.37 A per wire, the highest temperature rise lies within 46 degrees Celsius in respect to the surrounding environment temperature. These estimations are made with assumption that both external layers (1^{st} and 21^{st}) have a contact with metal plane (vacuum tube shell from one side and some cover from another). Images with results given by the program for some critical layers are shown in FIG. 6, FIG. 7 and FIG. 8. Note, that the surrounding environment is supposed to be "static" air. Using of fans or water as a cooler would apparently allow to decrease temperature rise.

IV. SUMMARY

On the basis of multipole expansion of potential, the angular distribution of electrical current on the circular surface was found analytically. This result was used to build a program that creates the model of PCB coil, which induces multipole magnetic field with given parameters. The analysis showed, that the coil for the focusing optics with parameters, which were intended to be used on IOTA ring, would had to be built with too many turns and, thus, is not realistic. Moreover, it was decided to use only octupole field in order to reduce the number of total turns. Nevertheless, it was possible to develop a model of realistic coil with minimum changes in initial options of the focusing optics. Such coil consists of 21

TABLE II. Description of octupole coil

Parameter	**Sign**	**Value**	**Comment**
Vacuum tube radius	r_d	0.5 in.	reduced twice
Constant c	c	0.02 $\sqrt{\text{m}}$	enlarged twice
Peak current	I_4	201.18 A	
Length of the sector	l_a	10 mm	arc on the tube surface corresponding to the cosine half-length
Length of the section		2 mm	$l_a/5$
Wire "height"	h	0.035 mm	depth of copper foil
Wire width	w	0.254 mm	
Wire current[a]	I_w	0.37 A	
Dissipated power		630 W/m	Total power dissipated by whole coil
Max number of wires per section	n_i	4	
Number of turns	N	21	
Number of unique layers		4	
Total coil thickness		1.8 mm	

[a] Under the current of 0.4 A, the wire with such height and width will be heated on $10°C$ in static air atmosphere. Value taken from Flex-Circuit Design Guide made by one of PCB developer http://www.temflexcontrols.com/pdf/aa24.pdf

layers and should be powered by 0.37 A current source. Calculations performed with help of special software show, that such electrical current would cause 46 °C temperature rise, which is not critical and can be cooled down.

ACKNOWLEDGMENTS

This work was carried out within the PARTI summer internship program at Fermilab. I would like to express the deepest appreciation to my supervisor Alexander Valishev, for his valuable help with my introduction to accelerator physics, a lot of beneficial advices during the work and help with editing this text. I would also like to thank Leo Michelloti, for his

TABLE III. Wire distribution in one sector of the coil with parameters from table II

Layers	**Sec1**	**Sec2**	**Sec3**	**Sec4**	**Sec5**
1-6	4	4	4	4	4
7	2	4	4	4	2
8-17	0	4	4	4	0
18-21	0	0	4	0	0

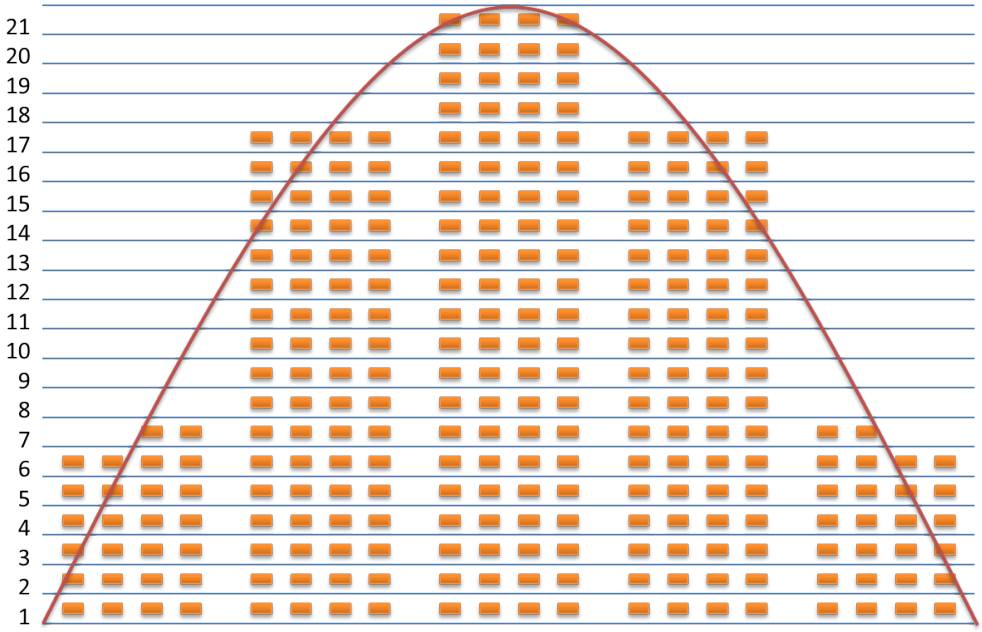

FIG. 5. A scheme of wires location in one sector (cross-section). Small rectangles represent single wires, horizontal lines separate different layers.

inspirational lectures.

[1] V. Danilov and S. Nagaitsev, Nonlinear accelerator lattices with one and two analytic invariants, Phys. Rev. ST Accel. Beams **13**, 084002 (2010).

[2] S. Nagaitsev and V. Danilov, A Search for Integrable Four-dimensional Nonlinear Accelerator Lattices, Proceedings of IPAC'10, Kyoto, Japan, THPE094 (2010).

[3] A. Valishev et al., Beam Physics of Integrable Optics Test Accelerator at Fermilab, FERMILAB-CONF-12-209-AD-APC

[4] D. Shatilov, https://indico.fnal.gov/conferenceDisplay.py?confId=5151

[5] Saturn PCB Design Toolkit, http:////www.saturnpcb.com//pcb_toolkit.htm

TABLE IV. Different variants of octupole coils.

r_d, mm	l_a, mm	w, mm	n_i	h, mm	I_w, A	$c, \sqrt{m}$	I_4, A	N
25.4	20	0.25	8	35	0.4	0.01	12876	622
25.4	20	0.25	8	70	0.6	0.01	12876	415
25.4	20	0.25	8	105	0.8	0.01	12876	311
25.4	20	0.5	4	35	0.6	0.01	12876	829
25.4	20	0.5	4	70	1.1	0.01	12876	454
25.4	20	0.5	4	105	1.5	0.01	12876	332
25.4	20	0.25	8	35	0.4	0.02	3219	156
25.4	20	0.25	8	70	0.6	0.02	3219	104
25.4	20	0.25	8	105	0.8	0.02	3219	78
25.4	20	0.5	4	35	0.6	0.02	3219	208
25.4	20	0.5	4	70	1.1	0.02	3219	115
25.4	20	0.5	4	105	1.5	0.02	3219	83
25.4	20	0.25	8	35	0.4	0.03	1430	70
25.4	20	0.25	8	70	0.6	0.03	1430	47
25.4	20	0.25	8	105	0.8	0.03	1430	35
25.4	20	0.5	4	35	0.6	0.03	1430	93
25.4	20	0.5	4	70	1.1	0.03	1430	51
25.4	20	0.5	4	105	1.5	0.03	1430	37
25.4	20	0.25	8	35	0.4	0.04	804	39
25.4	20	0.25	8	70	0.6	0.04	804	26
25.4	20	0.25	8	105	0.8	0.04	804	20
25.4	20	0.5	4	35	0.6	0.04	804	52
25.4	20	0.5	4	70	1.1	0.04	804	29
25.4	20	0.5	4	105	1.5	0.04	804	21

r_d, mm	l_a, mm	w, mm	n_i	h, mm	I_w, A	$c, \sqrt{m}$	I_4, A	N
12.7	10	0.25	4	35	0.4	0.01	804	78
12.7	10	0.25	4	70	0.6	0.01	804	52
12.7	10	0.25	4	105	0.8	0.01	804	39
12.7	10	0.5	2	35	0.6	0.01	804	104
12.7	10	0.5	2	70	1.1	0.01	804	57
12.7	10	0.5	2	105	1.5	0.01	804	42
12.7	10	0.25	4	35	0.4	0.02	201	20
12.7	10	0.25	4	70	0.6	0.02	201	13
12.7	10	0.25	4	105	0.8	0.02	201	10
12.7	10	0.5	2	35	0.6	0.02	201	26
12.7	10	0.5	2	70	1.1	0.02	201	15
12.7	10	0.5	2	105	1.5	0.02	201	11
12.7	10	0.25	4	35	0.4	0.03	89	9
12.7	10	0.25	4	70	0.6	0.03	89	6
12.7	10	0.25	4	105	0.8	0.03	89	5
12.7	10	0.5	2	35	0.6	0.03	89	12
12.7	10	0.5	2	70	1.1	0.03	89	7
12.7	10	0.5	2	105	1.5	0.03	89	5
12.7	10	0.25	4	35	0.4	0.04	50	5
12.7	10	0.25	4	70	0.6	0.04	50	4
12.7	10	0.25	4	105	0.8	0.04	50	3
12.7	10	0.5	2	35	0.6	0.04	50	7
12.7	10	0.5	2	70	1.1	0.04	50	4
12.7	10	0.5	2	105	1.5	0.04	50	3

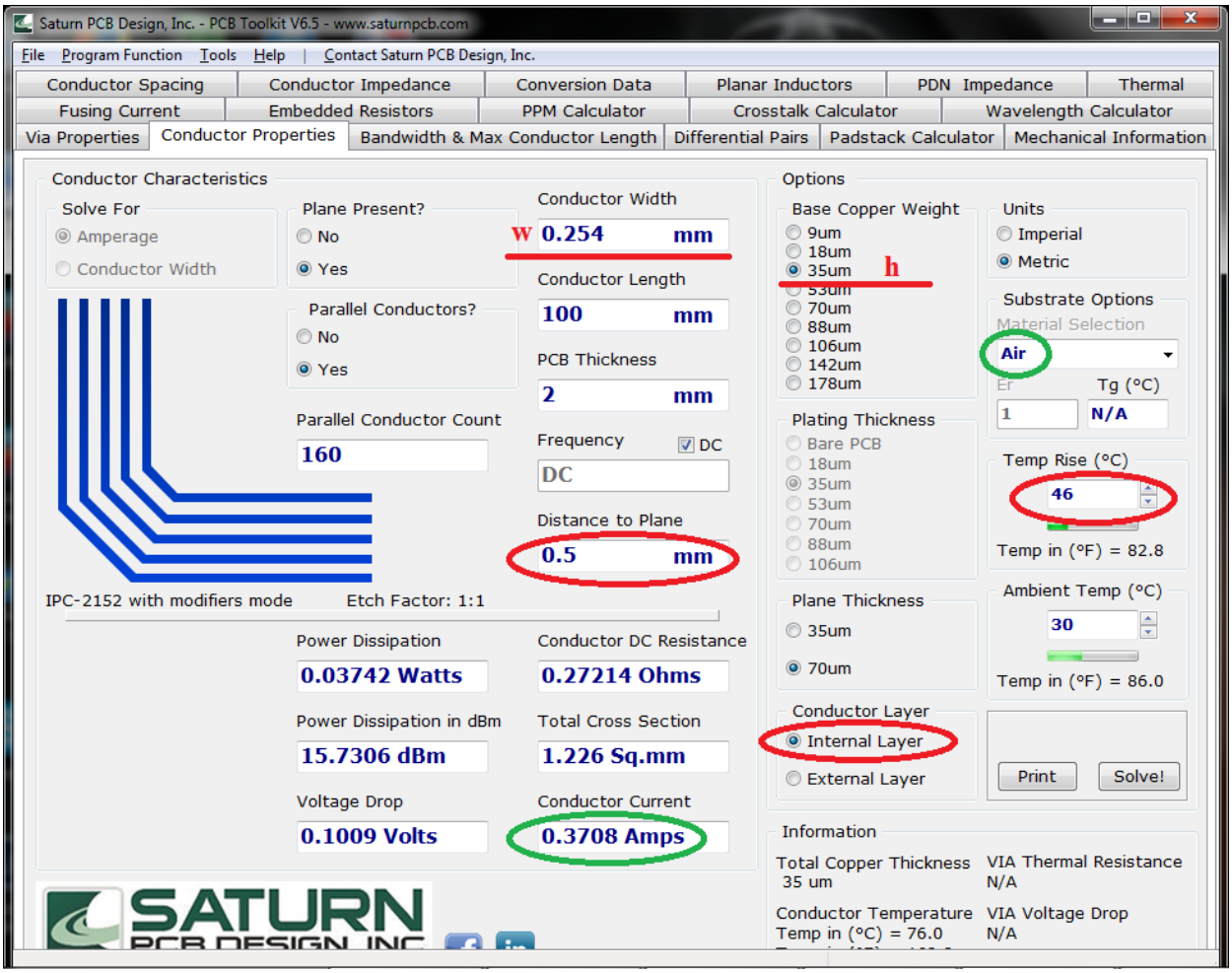

FIG. 6. Estimation of temperature rise for the 6^{th} layer of the coil model (see FIG. 5). This layer is under the highest heating of all others due to fact that it is internal and has a large number of wires in it. Nonetheless, temperature rise is 46 degrees Celsius for the current 0.37 A. Height h and width w of conductors are chosen the same as in the model described above. The number of the layer is defined by the distance to metal plane (0.5 mm), which is supposed to be the shell of vacuum tube.

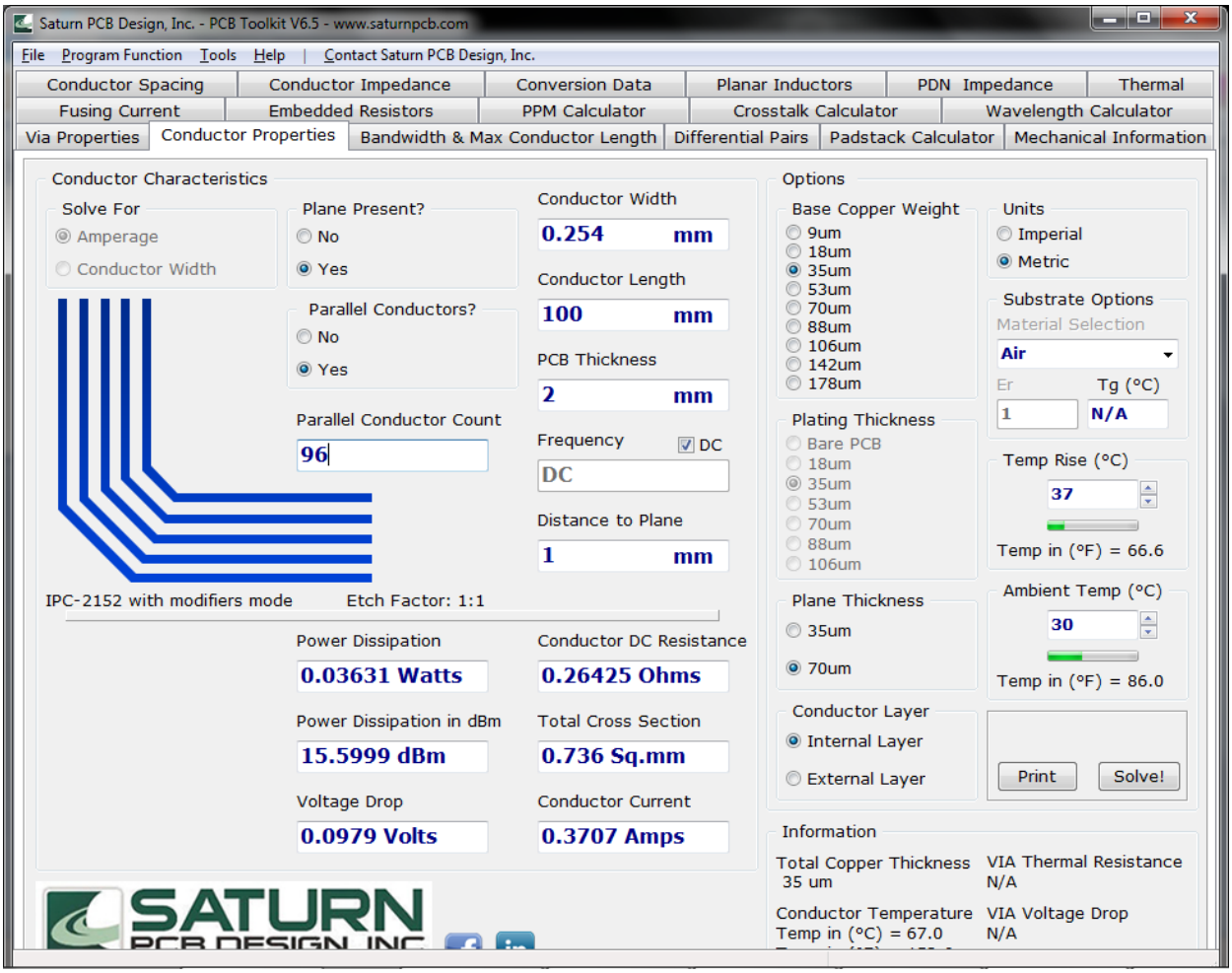

FIG. 7. Estimation of temperature rise for the 11^{th} layer of the coil model (see FIG. 5). This layer is in the middle of all coil. Temperature rise is 37 degrees Celsius for the current 0.37 A, which is lower than the 6^{th} layer has (FIG.6). Height h and width w of conductors are chosen the same as in the model described above. The number of the layer is defined by the distance to metal plane (1 mm), which is supposed to be the shell of vacuum tube.

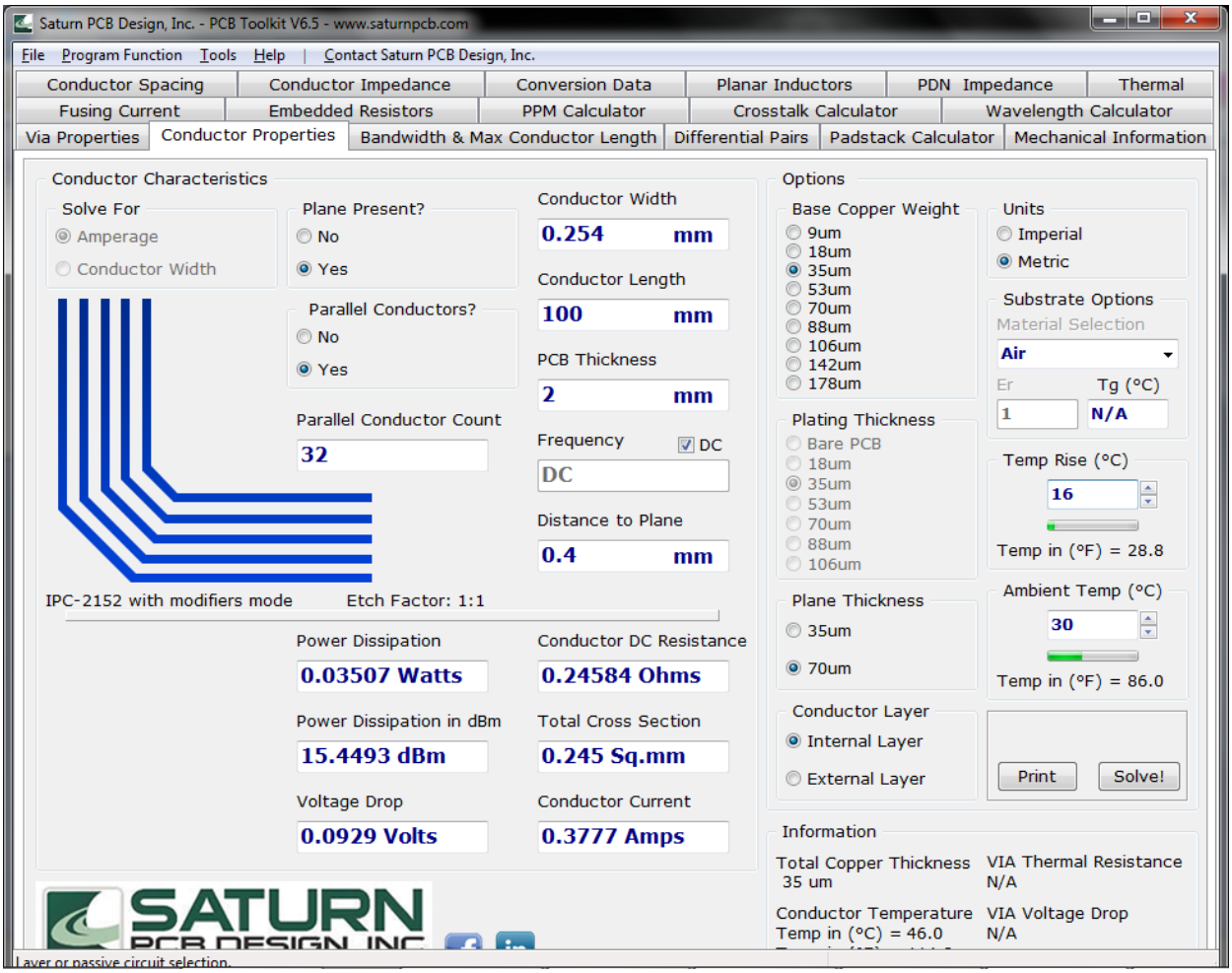

FIG. 8. Estimation of temperature rise for the 18^{th} layer of the coil model (see FIG. 5). This layer is on of the those which have the lowest number of conductors. Temperature rise is just 16 degrees Celsius for the current a little bit more than 0.37 A. Height h and width w of conductors are chosen the same as in the model described above. The number of the layer is defined by the distance to metal plane (0.4 mm), which is supposed to be the outer cover.